Macrophage Migration Inhibitory Factor as a Chaperone Inhibiting Accumulation of Misfolded SOD1

Highlights

- A cytosolic chaperone inhibits ALS-causing mutant SOD1 binding to mitochondria and ER

- An unbiased screen identifies inhibition by MIF of ALS-causing mutant SOD1 misfolding

- Direct action of the ATP-independent chaperone activity of MIF reduces misfolded SOD1

- Elevation of MIF levels extends survival of mutant SOD1-expressing motor neurons

Authors

Adrian Israelson, Dara Ditsworth, ..., Sandrine Da Cruz, Don W. Cleveland

Correspondence

adriani@bgu.ac.il (A.I.),
dcleveland@ucsd.edu (D.W.C.)

In Brief

Israelson et al. identify MIF as a chaperone inhibiting misfolding of ALS-linked SOD1 mutant proteins. Elevating MIF suppresses mutant SOD1 association with intracellular organelles and extends survival of mutant SOD1-expressing motor neurons, supporting therapies to enhance intracellular MIF chaperone activity.

CrossMark

CellPress

Macrophage Migration Inhibitory Factor as a Chaperone Inhibiting Accumulation of Misfolded SOD1

Adrian Israelson,[1,*] Dara Ditsworth,[2,3] Shuying Sun,[2,3] SungWon Song,[6,7] Jason Liang,[2] Marian Hruska-Plochan,[4,9] Melissa McAlonis-Downes,[2] Salah Abu-Hamad,[1] Guy Zoltsman,[1] Tom Shani,[1] Marcus Maldonado,[2] Anh Bui,[2] Michael Navarro,[4] Huilin Zhou,[2,3] Martin Marsala,[4] Brian K. Kaspar,[6,7,8] Sandrine Da Cruz,[2] and Don W. Cleveland[2,3,5,*]
[1]Department of Physiology and Cell Biology, Faculty of Health Sciences and The Zlotowski Center for Neuroscience, Ben-Gurion University of the Negev, P.O. Box 653, Beer Sheva 84105, Israel
[2]Ludwig Institute for Cancer Research
[3]Department of Cellular and Molecular Medicine
[4]Department of Anesthesiology
[5]Department of Neuroscience
University of California at San Diego, La Jolla, CA 92093-0670, USA
[6]The Research Institute at Nationwide Children's Hospital
[7]Molecular, Cellular and Developmental Biology Graduate Program
[8]Department of Neuroscience
The Ohio State University, Columbus, OH 43205, USA
[9]Present address: Institute of Molecular Life Sciences, University of Zurich, Y32-J06, Winterthurerstrasse 190, 8057 Zurich, Switzerland
*Correspondence: adriani@bgu.ac.il (A.I.), dcleveland@ucsd.edu (D.W.C.)
http://dx.doi.org/10.1016/j.neuron.2015.02.034

SUMMARY

Mutations in superoxide dismutase (SOD1) cause amyotrophic lateral sclerosis (ALS), a neurodegenerative disease characterized by loss of motor neurons and accompanied by accumulation of misfolded SOD1 onto the cytoplasmic faces of intracellular organelles, including mitochondria and the endoplasmic reticulum (ER). Using inhibition of misfolded SOD1 deposition onto mitochondria as an assay, a chaperone activity abundant in nonneuronal tissues is now purified and identified to be the multifunctional macrophage migration inhibitory factor (MIF), whose activities include an ATP-independent protein folding chaperone. Purified MIF is shown to directly inhibit mutant SOD1 misfolding. Elevating MIF in neuronal cells suppresses accumulation of misfolded SOD1 and its association with mitochondria and the ER and extends survival of mutant SOD1-expressing motor neurons. Accumulated MIF protein is identified to be low in motor neurons, implicating correspondingly low chaperone activity as a component of vulnerability to mutant SOD1 misfolding and supporting therapies to enhance intracellular MIF chaperone activity.

INTRODUCTION

Amyotrophic lateral sclerosis (ALS) is a progressive adult-onset neurodegenerative disorder characterized by the selective loss of upper and lower motor neurons. About 10% are inherited in a dominant manner (Da Cruz and Cleveland, 2011), with 20% of familial cases caused by mutation of cytoplasmic Cu/Zn superoxide dismutase (SOD1) (Rosen et al., 1993). The exact mechanism(s) responsible for motor neuron degeneration remains unsettled, albeit models for each of the nine most prominently proposed pathways include damage from misfolded, mutant SOD1 (Ilieva et al., 2009).

Multiple groups have identified that SOD1 mutants with divergent biochemical characteristics share a common property, with a proportion of the predominantly cytosolic SOD1 being localized to mitochondria (Israelson et al., 2010; Liu et al., 2004; Mattiazzi et al., 2002; Vande Velde et al., 2008) and/or the ER (Fujisawa et al., 2012; Nishitoh et al., 2008) but only in nervous system tissues in patient samples and rodent models. In particular, misfolded mutant SOD1 association with derlin-1, a component of the ER-associated degradation pathway, has been implicated in induction of ER stress from disrupted removal of misfolded proteins from the ER (Fujisawa et al., 2012; Nishitoh et al., 2008). Derlin-1 is bound by at least 132 of the ALS-linked SOD1 mutants, each of which exposes a derlin-1-binding domain buried in correctly folded SOD1 (Fujisawa et al., 2012).

Purification of mitochondria, including floatation steps that eliminate protein-only aggregates, has demonstrated that mutant SOD1 deposition occurs on the cytoplasmic face of the outer membrane of spinal cord mitochondria (Liu et al., 2004; Vande Velde et al., 2008), accompanied by altered mitochondrial shape and distribution (Vande Velde et al., 2011). These findings were reinforced by demonstration (using sensitivity to proteolysis and immunoprecipitation with an antibody specific for misfolded SOD1) that misfolded forms of both dismutase active and inactive mutant SOD1 are deposited onto the cytoplasmic
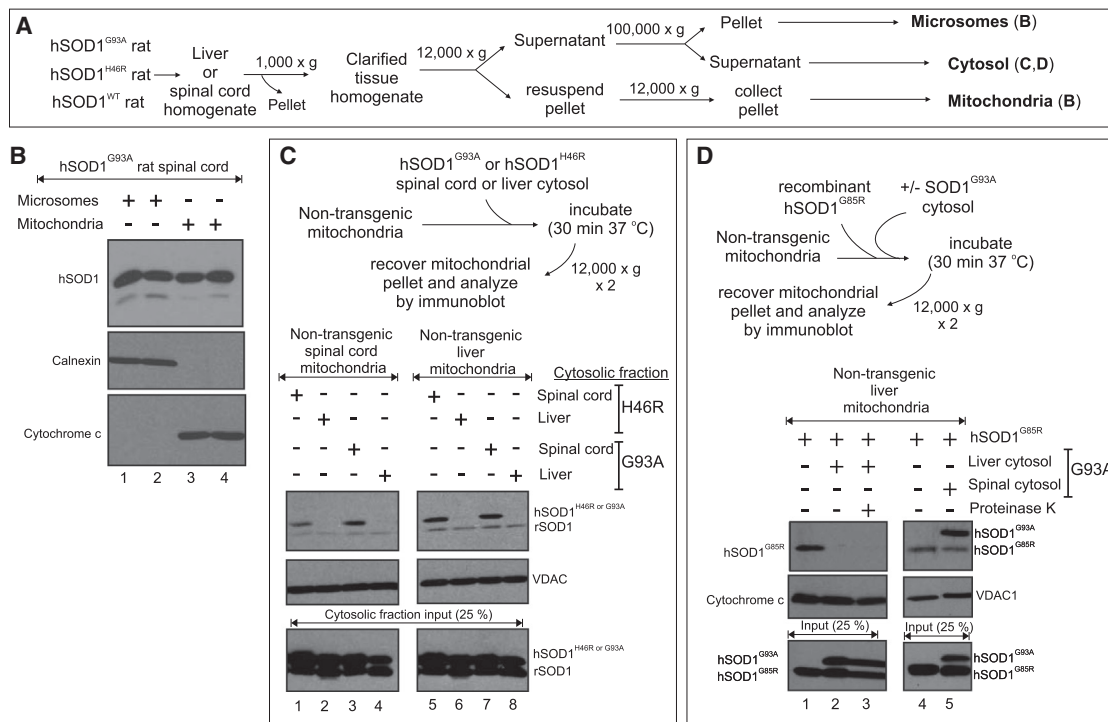
Figure 1. The Cytosol Determines Mutant SOD1 Association with Mitochondria

(A) Schematic outlining purification steps for isolation of microsomes, cytosol, and mitochondria from liver or spinal cord.

(B) Immunoblot assay for mutant SOD1 associated with microsomes or mitochondria purified as in (A) from SOD1^{G93A} rat spinal cord. Calnexin and cytochrome c immunoblots were used as specific markers for microsomal and mitochondrial fractions, respectively.

(C) Cytosol from SOD1^{G93A}- or SOD1^{H46R}-expressing rats was incubated with nontransgenic spinal cord- or liver-derived mitochondria, and the mitochondria were recovered and analyzed by immunoblotting for bound mutant SOD1. Immunoblotting for VDAC1 was used to verify numbers of mitochondria recovered from each assay. Bottom: input cytosols were immunoblotted to identify the initial levels of human mutant SOD1 and endogenous rat SOD1.

(D) Recombinant mutant SOD1^{G85R} was incubated with nontransgenic liver mitochondria in the absence or presence of liver or spinal cord cytosol from SOD1^{G93A} rats. Mitochondria were recovered and assayed by immunoblotting for whether addition of spinal cord or liver cytosol affected recruitment of SOD1^{G85R} to mitochondria. Mitochondrial recovery was assessed by immunoblotting for VDAC1 or cytochrome c. The two lanes from the right panel were not loaded in the same order as shown.

face of the outer membrane of spinal cord mitochondria (Vande Velde et al., 2008). One component directly bound by misfolded SOD1 is voltage-dependent anion channel-1 (VDAC1), with binding inhibiting its conductance of adenine nucleotides across the outer mitochondrial membrane (Israelson et al., 2010). Moreover, mutant SOD1 may also interact with other components of the mitochondrial outer membrane, including Bcl-2 (Pedrini et al., 2010) and the protein import machinery (Li et al., 2010), thereby altering the corresponding activities.

Recognizing that expression of SOD1 is ubiquitous but misfolded SOD1 accumulation and binding to mitochondria and the ER are found only in nervous system tissues, one of the most important unsolved questions is the molecular mechanism(s) underlying cell-type selectivity for accumulation of misfolded SOD1 and its association with intracellular organelles. Here we purify a cytosolic activity whose action inhibits mutant SOD1 misfolding onto mitochondria and the ER. We identify this factor to be macrophage migration inhibitory factor (MIF), a multifunctional protein whose activities include an ATP-independent protein folding chaperone (Cherepkova et al., 2006). We propose that a low MIF level within motor neurons is one

component of their selective vulnerability to ubiquitously expressed mutations in SOD1.

RESULTS

The Cytosol Determines Mutant SOD1 Association with Mitochondria and the ER

We previously reported that ALS-causing mutant SOD1 association with mitochondria was characterized by misfolded SOD1 binding to components, including VDAC1, on the outer mitochondrial membrane but was found for mitochondria isolated from spinal cord but not for those similarly purified from liver (Israelson et al., 2010). Consistent with this and other reports, immunoblot analysis of microsomes or mitochondria isolated from spinal cord homogenates (see schematic in Figure 1A) from rats expressing either of two ALS-linked mutations in SOD1 (SOD1^{G93A} [Howland et al., 2002] and SOD1^{H46R} [Nagai et al., 2001]) revealed that mutant SOD1 bound both to microsomal and mitochondrial membranes (Figure 1B). To determine whether this selective association of mutant SOD1 with spinal mitochondria was mediated by the spinal cord mitochondria or
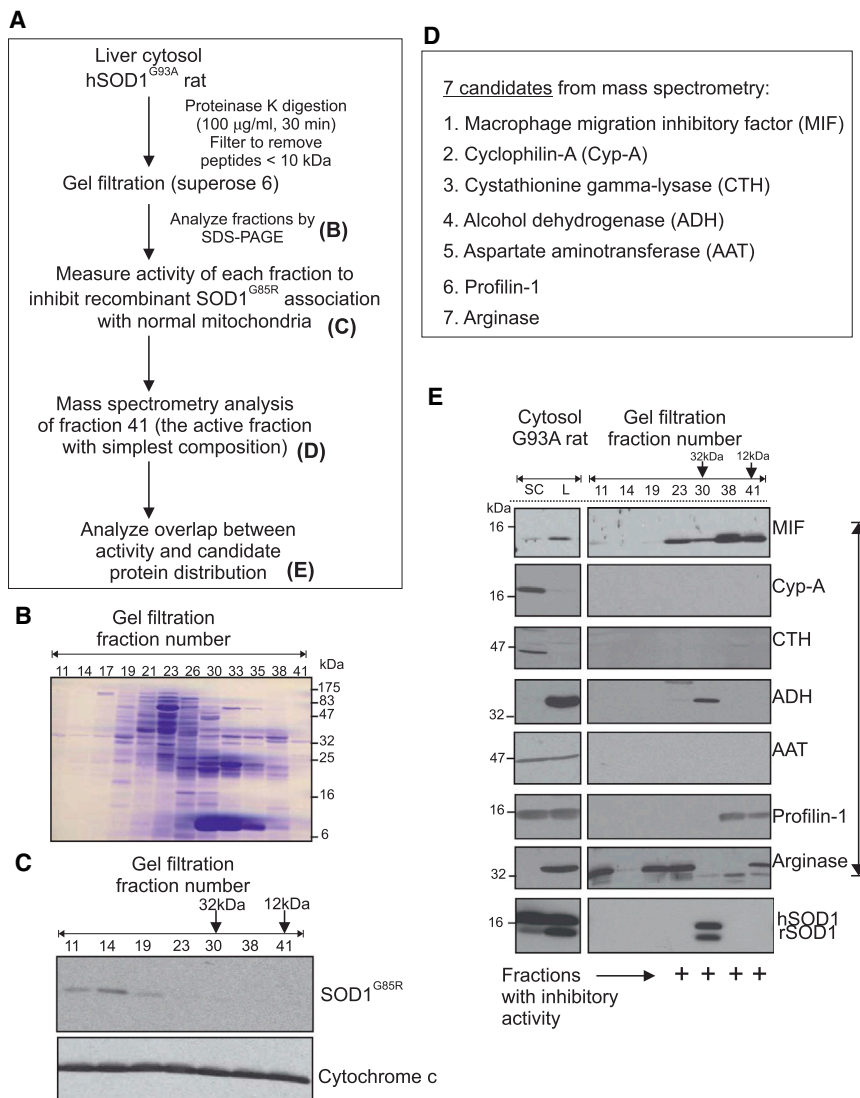
A

Liver cytosol
hSOD1^{G93A} rat

↓ Proteinase K digestion
(100 μg/ml, 30 min)
Filter to remove
peptides < 10 kDa

Gel filtration (superose 6)

↓ Analyze fractions by
SDS-PAGE **(B)**

Measure activity of each fraction to
inhibit recombinant SOD1^{G85R} association
with normal mitochondria **(C)**

↓

Mass spectrometry analysis
of fraction 41 (the active fraction
with simplest composition) **(D)**

↓

Analyze overlap between
activity and candidate
protein distribution **(E)**

B

Gel filtration
fraction number

11 14 17 19 21 23 26 30 33 35 38 41   kDa

—175
—83
—47
—32
—25
—16
—6

C

Gel filtration
fraction number

32kDa   12kDa
↓   ↓
11   14   19   23   30   38   41

SOD1^{G85R}

Cytochrome c

D

7 candidates from mass spectrometry:

1. Macrophage migration inhibitory factor (MIF)
2. Cyclophilin-A (Cyp-A)
3. Cystathionine gamma-lysase (CTH)
4. Alcohol dehydrogenase (ADH)
5. Aspartate aminotransferase (AAT)
6. Profilin-1
7. Arginase

E

Cytosol   Gel filtration
G93A rat   fraction number

32kDa 12kDa
SC L   11 14 19 23 30 38 41

kDa
16 —   MIF
16 —   Cyp-A
47 —   CTH
32 —   ADH
47 —   AAT
16 —   Profilin-1
32 —   Arginase
16 —   hSOD1
                                  rSOD1

Fractions ⟶ + + + +
with inhibitory
activity

Figure 2. Identification of MIF as Having an Activity that Can Suppress Mutant SOD1 Association with Mitochondria

(A) Schematic outlining the purification steps of an activity in liver cytosol that inhibits mutant SOD1 association with normal mitochondria, followed by mass spectrometry to identify remaining proteins.

(B) Coomassie staining of an SDS-polyacrylamide gel of gel filtration fractions from (A).

(C) Assay of gel filtration fractions from (A) and (B) for the presence of an activity that inhibits association of recombinant mutant SOD1^{G85R} with normal liver mitochondria.

(D) The seven proteins identified by mass spectrometry to be present within gel filtration fraction 41 from (C), which contained activity inhibiting recombinant SOD1 binding to nontransgenic liver mitochondria and had the simplest protein composition.

(E) Immunoblotting of gel filtration fractions for the presence of each of the seven candidate proteins identified in (D). Only MIF cofractionated with inhibitory activity. SC, spinal cord; L, liver.

Next, we investigated whether there was a factor(s) in spinal cord cytosol that induced association of SOD1 with normal mitochondria or, in contrast, whether some factor in the liver prevented binding. To do this, recombinant SOD1^{G85R} was incubated with mitochondria purified from liver of nontransgenic rats in the presence of SOD1^{G93A} spinal cord or liver extract. Whereas spinal cord cytosol did not affect SOD1^{G85R} association with mitochondria (Figure 1D, lane 5), added liver cytosol inhibited it (Figure 1D, compare lanes 1 and 2). This inhibitory activity was not affected by inhibitors of the Hsp70 and Hsp90 protein chaperones and was independent of calcium (Figure S1). Remarkably, although the inhibitory activity was heat labile (consistent with a protein activity), it was not inactivated by degradation of most proteins by incubation of the liver cytosol with proteinase K (Figure 1D, lane 3).

Identification of MIF as an Inhibitor of Mutant SOD1 Association with Mitochondria

To identify the activity responsible for blocking association of mutant SOD1 with mitochondria, liver cytosol was incubated with proteinase K and the resultant peptides and other low-molecular-weight species below 10 kDa were removed by centrifugal filtration. Remaining proteins and other macromolecules were then fractionated by gel permeation chromatography (see schematic in Figure 2A). Finally, fractions were assayed for the ability to inhibit recombinant SOD1^{G85R} binding to nontransgenic mitochondria. Activity eluted broadly with apparent molecular weights between 12 and 45 kDa. Proteins in the fractions with activity (fractions 23–41; Figure 2C) were visualized by PAGE

the corresponding cytosol, we isolated normal, nontransgenic mitochondria from spinal cord and liver. Those mitochondria were then incubated (Figure 1C) with cytosolic extracts prepared (as in Figure 1A) from spinal cords or livers of rats expressing dismutase active (SOD1^{G93A}) or inactive (SOD1^{H46R}) mutants.

The mitochondria were reisolated and analyzed by immunoblotting for mutant SOD1. Although the liver and spinal cord cytosols contained comparable levels of mutant human SOD1 (Figure 1C, bottom), none of the mutant SOD1 in liver cytosol bound to liver- or spinal cord-derived nontransgenic mitochondria. In contrast, incubation with spinal cord cytosols from SOD1^{G93A}- or SOD1^{H46R}-expressing rats did yield association of a proportion of both mutant SOD1s with wild-type mitochondria. For both dismutase active (SOD1^{G93A}) and inactive (SOD1^{H46R}) mutants, binding was independent of the tissue from which the mitochondria were isolated (Figure 1C). Thus, the tissue origin of the cytosol, not of the mitochondrion, determines whether mutant SOD1 in those cytosols binds to mitochondria.

and Coomassie staining (Figure 2B). The most slowly eluting fraction with activity (fraction 41) had only a handful of observable polypeptides (Figure 2B). We therefore used mass spectrometry to analyze its protein content. Although the sensitivity of mass spectrometry frequently identifies many proteins present in such assays, remarkably, however, only seven proteins were detected (Figure 2D). One of these, profilin-1, an actin-binding protein linked to regulation of actin polymerization, was notable, as mutations in it are causative of a small proportion of inherited ALS (Wu et al., 2012). Nevertheless, immunoblotting was used to determine that profilin-1 was absent from many fractions (23–30) that retained inhibitory activity (Figure 2E).

Similar immunoblotting with antibodies to each of the six remaining proteins determined that only one cofractionated with the inhibitory activity (Figure 2E). This was the 12-kDa macrophage migration inhibitory factor, which has previously been implicated in divergent functional roles: as a protein folding chaperone (Cherepkova et al., 2006), thiol-oxidoreductase protein (Kleemann et al., 1998), and secreted cytokine with an important role in innate immunity (Calandra and Roger, 2003; Lolis and Bucala, 2003). MIF eluted broadly in fractions spanning from 12 to 45 kDa apparent molecular weights, just as did the activity for inhibiting mutant SOD1 binding to mitochondria. The broad elution of MIF was not because of poor resolution of the column, as other proteins (including alcohol dehydrogenase, profilin-1, and SOD1 itself) fractionated much more sharply. Rather, the broad elution was fully consistent with MIF's known ability to form dimers and trimers (Mischke et al., 1998; Philo et al., 2004) through an exposed hydrophobic face as a part of its ATP-independent activity as a protein folding chaperone (Cherepkova et al., 2006). Interestingly, MIF protein levels do not change within the spinal cord during disease course in SOD1 mutant mice (Figure S2).

Dose-Dependent Inhibition by MIF of Mutant SOD1 Association with Mitochondria

As a direct test of whether MIF inhibits association of mutant SOD1 with mitochondria, purified mutant or wild-type SOD1 (Figure 3A, bottom right) was added to normal liver mitochondria in the presence or absence of purified MIF (see schematic in Figure 3A). After recovering the mitochondria by centrifugation, immunoblotting was used to reveal that a proportion of SOD1^{G93A} and SOD1^{G85R}, but not SOD1^{WT}, bound to nontransgenic mitochondria in a dose-dependent manner (Figure S3) in the absence of MIF (Figure 3B). Mutant SOD1 binding was inhibited in a dose-dependent manner by coincubation with MIF, with a 1:80 molar ratio of MIF to SOD1 (50 ng of MIF and 4 μg of mutant SOD1), sufficient to strongly diminish (by >90%) binding of mutant SOD1 to mitochondria (Figure 3C). Importantly, about 5%–10% of recombinant mutant SOD1 bound to mitochondria in these assays (Figure 3C), a percentage of misfolded SOD1 similar to that measured in immunoprecipitates of the initial recombinant SOD1 preparation when using B8H10 antibodies that bind misfolded SOD1 (Figure S5).

We exploited the known proteinase K resistance or sensitivity, respectively, of correctly folded and misfolded SOD1^{G93A} (Borchelt et al., 1994; Ratovitski et al., 1999) to test whether the mutant SOD1 that associates with mitochondria represents the initially misfolded fraction. We initially verified that most of the dismutase active SOD1^{G93A} is protease resistant; in contrast, most of the inactive SOD1^{G85R} was sensitive (Figure 3E). SOD1^{G93A} was preincubated with proteinase K, the protease was then inactivated by addition of PMSF and the mixture was incubated with normal liver mitochondria, and finally mitochondria along with any bound mutant SOD1 were recovered by centrifugation. Immunoblotting for human SOD1 demonstrated that SOD1^{G93A} association with mitochondria was completely eliminated by proteinase K preincubation, confirming that the protease-sensitive, misfolded fraction is the one that associates with mitochondria (Figure 3D).

Inhibition of misfolded SOD1 association with mitochondria was specific to MIF, as other chaperones tested, including Hsp27, Hsc70, aB-crystallin (previously reported to interact with mutant and misfolded SOD1 and modulate its aggregation; Karch and Borchelt, 2010; Krishnan et al., 2008; Wang et al., 2005, 2009; Yerbury et al., 2013; Zetterström et al., 2011b), cyclophilin-A (one of our seven candidate proteins and previously proposed to act as a chaperone; Freskgård et al., 1992), or glutathione peroxidase (a protein with thiol-oxidoreductase activity, an activity that has been proposed to be crucial for the association of mutant SOD1 proteins with mitochondria; Cozzolino et al., 2008; Ferri et al., 2006), had no effect on mutant SOD1 association with normal mitochondria (Figures 3F and 3G).

MIF Suppresses Misfolded Mutant SOD1 Association with ER and Mitochondrial Membranes in Motor Neuron-like Cells

We next tested whether MIF inhibited association of mutant SOD1 not only with mitochondria but also with other intracellular membranes in motor neuron-like (NSC-34) cells expressing ALS-linked SOD1 mutants (see schematic in Figure 4A). EGFP-tagged SOD1^{G93A} or SOD1^{G85R} was expressed by DNA transfection, along with lower or higher amounts of MIF. Accumulated levels were validated by immunoblotting for each protein (Figure 4B, bottom), and the association of mutant SOD1 with ER membranes was determined after isolation of microsomes. Both dismutase active (SOD1^{G93A}) and dismutase inactive (SOD1^{G85R}) mutants bound to ER membranes in the presence of the low endogenous levels of MIF (Figure 4B, lanes 1 and 4), but binding in both cases was reduced in a dose-dependent manner when MIF levels were elevated (Figure 4B). MIF also inhibited mutant SOD1 association with mitochondria (Figure 4C).

We next tested whether MIF also inhibited accumulation of misfolded SOD1 in a dose-dependent manner in the same motor neuron-like cells expressing ALS-linked SOD1 mutants (see schematic in Figure 4D). In the absence of transfected MIF, misfolded SOD1 accumulated and could be detected by immunoprecipitation with the B8H10 antibody, which does not recognize wild-type SOD1 but does recognize a wide spectrum of misfolded SOD1 mutants (Gros-Louis et al., 2010) including SOD1^{G93A} and SOD1^{G85R} (Figure 4E, lanes 2 and 3). Transfection to simultaneously express MIF along with either SOD1^{G93A} or SOD1^{G85R} reduced the level of misfolded SOD1 (Figure 4E, lanes 4 and 5), without affecting the overall level of accumulated mutant SOD1. Similar results were observed by expressing
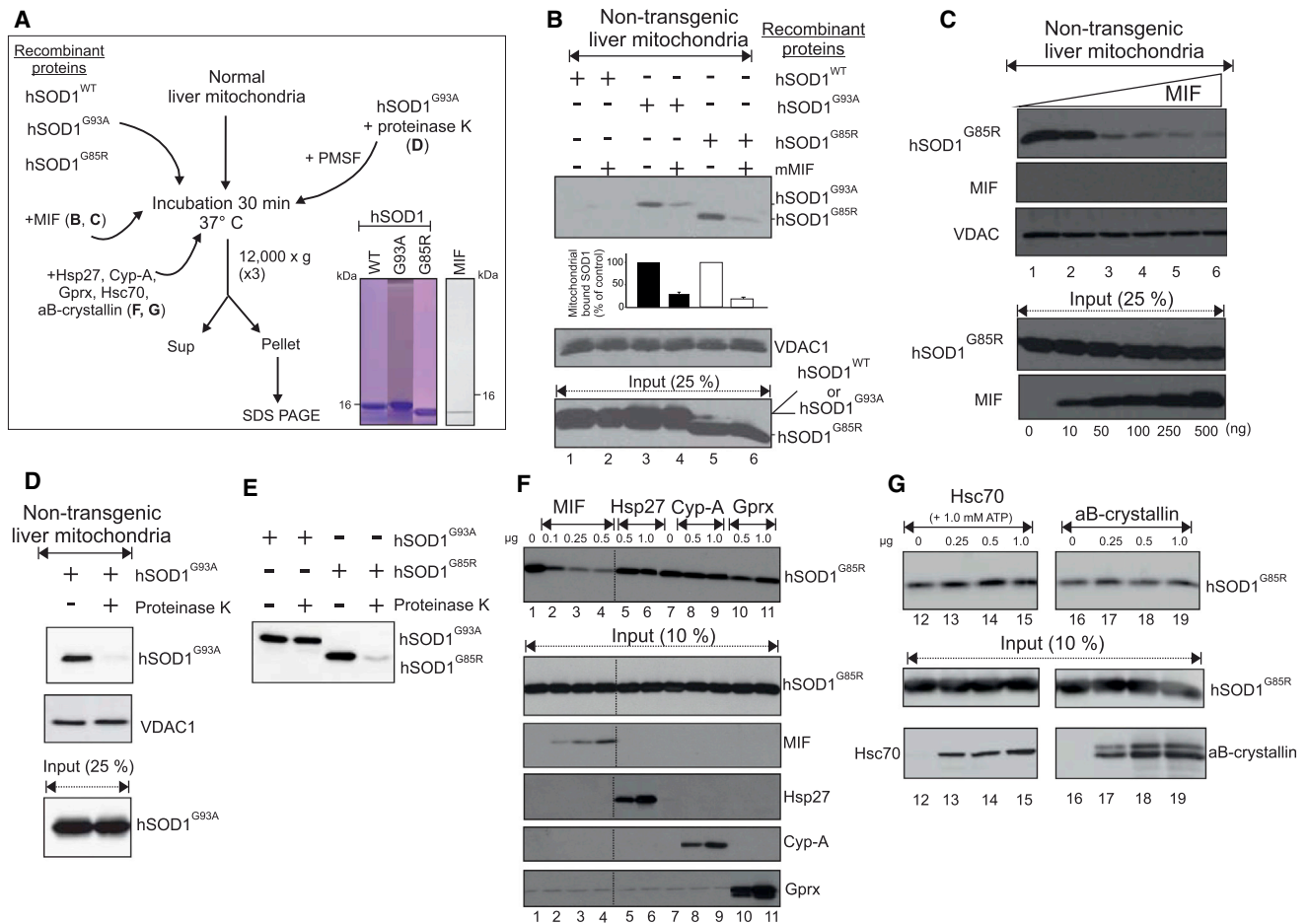
Figure 3. Recombinant MIF Inhibits Association of Mutant SOD1 with Mitochondria in a Dose-Dependent Manner
(A) Schematic of a protocol to test whether purified recombinant MIF inhibits association of recombinant SOD1^{G85R} or SOD1^{G93A} with normal liver mitochondria. Lower right: Coomassie-stained SDS-polyacrylamide gel analysis of recombinant SOD1 and MIF.
(B) Immunoblotting of mitochondria recovered from the protocol in (A) and assayed for MIF-dependent inhibition of association of either SOD1^{G85R} or SOD1^{G93A} when coincubated with nontransgenic liver mitochondria. Immunoblotting for VDAC1 was used to verify the amount of mitochondria added/recovered. Bar values represent the means ± SEM of three independent experiments.
(C) Immunoblot assay as in (A) for dose-dependent inhibition by recombinant MIF of mutant SOD1^{G85R} binding to nontransgenic liver mitochondria. Immunoblotting for VDAC1 was used to determine mitochondrial recovery. Immunoblotting for MIF was used to determine the absence of MIF in the mitochondrial fraction and the increased levels of MIF in the supernatant that were used.
(D) Immunoblotting of mitochondria recovered from the protocol in (A) and assayed for proteinase K-dependent inhibition of association of SOD1^{G93A} with nontransgenic liver mitochondria. Immunoblotting for VDAC1 was used to verify the amount of mitochondria added/recovered.
(E) Immunoblotting was used to determine the effect of proteinase K on recombinant SOD1^{G93A} or SOD1^{G85R}.
(F and G) Assay patterned after the protocol in (A) testing for whether purified (F) MIF, Hsp27, cyclophilin-A (Cyp-A), or glutathione peroxidase (Gprx) or (G) Hsc70 or aB-crystallin inhibits SOD1^{G85R} association with nontransgenic liver mitochondria. Some lanes were not loaded in the same order as shown in the figure.

MIF in the presence of untagged versions of SOD1^{G93A} or SOD1^{G85R} in human SH-SY5Y neuroblastoma cells (Figure S4).

The Thiol-Oxidoreductase Activity of MIF Is Not Necessary for Suppressing Misfolded SOD1

One of MIF's previously documented enzymatic roles is as a thiol-oxidoreductase (Kleemann et al., 1998). SOD1 monomers lacking the C57-C146 disulfide bond represent the major portion of misfolded SOD1 (Zetterström et al., 2013), thus suggesting that a thiol-oxidoreductase activity may play an important role in misfolded protein formation. To determine whether the action

of MIF in suppressing accumulation of misfolded SOD1 required this activity, cells were transfected with a point mutant of MIF (MIF^{C60S}) previously shown to completely lack oxidoreductase activity (Kleemann et al., 1998). Coexpression of MIF^{C60S} in NSC-34 cells with either SOD1^{G93A} or SOD1^{G85R} inhibited the accumulation of misfolded SOD1 in a dose-dependent manner (Figure 4F), consistent with an in vivo ability to suppress mutant SOD1 accumulation onto microsomal (Figure 4B) or mitochondrial membranes (Figure 4C). Misfolding of SOD1^{G93A}, which can acquire normal folding (as indicated by dimerization, protease resistance, and high specific activity as a superoxide

dismutase; Borchelt et al., 1994; Ratovitski et al., 1999), was more effectively suppressed by MIF[C60S] than was the dismutase inactive SOD1[G85R], most of which cannot adopt a stable conformation that confers protease resistance (Figure 3E).

MIF Directly Suppresses the Accumulation of Misfolded SOD1 In Vitro

To determine whether MIF directly inhibits the accumulation of misfolded SOD1, immunoprecipitation was performed (see schematic in Figure 5A) with a previously reported conformation-specific antibody (DSE2) that selectively recognizes misfolded, but not correctly folded, SOD1 (Israelson et al., 2010; Vande Velde et al., 2008). As expected, a proportion of SOD1[G93A] and SOD1[G85R], but not SOD1[WT], was immunoprecipitated with the DSE2 antibody (Figure 5B, lanes 3 and 5). Incubation of the mutant SOD1 with MIF nearly eliminated misfolded SOD1[G93A] that could be immunoprecipitated by DSE2 (Figure 5B, lane 3 versus 4). MIF also substantially inhibited accumulation of misfolded SOD1[G85R] (Figure 5B, lanes 5 and 6). Remarkably, a similar level of inhibition was observed when the SOD1[G85R] mutant was incubated with a liver cytosolic fraction that contained endogenous MIF accumulated to a similar level (Figure 5B, lane 7).

Next, purified SOD1[G93A] was depleted of initially misfolded SOD1 by immunoprecipitation with the B8H10 antibody (Figure 5D, lane 2), the unbound fraction free of misfolded SOD1 was incubated at 37°C in the absence (lane 3) or presence (lane 4) of MIF, and finally newly generated misfolded SOD1 was detected with a second round of immunoprecipitation with the B8H10 antibody. Remarkably, MIF suppressed formation of newly misfolded SOD1, as revealed by immunoblotting the final immunoprecipitate (Figure 5D, lane 4). Suppression was specific for MIF, because neither aB-crystallin nor Hsc70 (added at comparable concentrations) inhibited formation of newly misfolded SOD1 (Figure S6).

Possible direct binding of MIF to mutant SOD1 was tested by covalently labeling purified MIF with a green fluorescent dye (at a ratio of one labeled lysine residue per one MIF molecule) and incubating it with increasing concentrations of purified SOD1[G93A] (2.4 nM to 80 μM). Binding of the two was quantified using microscale thermophoresis, a sensitive protein-protein interaction assay (Wienken et al., 2010) that measures changes in the thermal migration behavior of particles in a temperature gradient as influenced by a binding partner. By plotting the percentage of change in normalized fluorescence as a function of SOD1[G93A] concentration (Wienken et al., 2010), curve fitting to the data points produced an excellent fit with a calculated dissociation constant (K_d) of 367 nM for interaction of mutant SOD1[G93A] and MIF (Figure 5E).

A Low Level of Endogenous MIF within Motor Neuron Perikarya

Immunostaining for MIF in nontransgenic rat spinal cord revealed it to be accumulated widely, with the striking exception of almost complete absence within choline acetyltransferase (ChAT)-positive motor neuron cell bodies (Figure 6A). In contrast, MIF was readily detected in astrocytes (Figure 6B). Although no change was apparent in overall MIF protein levels within the spi-

nal cord during disease course (Figure S2), immunostaining revealed increased MIF in reactive astrocytes just after symptomatic onset (i.e., 1 week after the first fibrillation) in a SOD1[G93A] rat (Figure 6D; Figure S7). Nevertheless, MIF protein remained undetectable in motor neurons, and this low level of intraperikaryal MIF was accompanied by accumulation of misfolded SOD1 (recognized by the B8H10 antibody) (Figures 6C and 6D; arrows in Figure 6E; Figure S7).

To determine whether the absence of accumulated MIF in motor neurons resulted from a low level (or absence) of synthesis of MIF in those neurons, we exploited bacTRAP reporter mouse lines (Doyle et al., 2008; Heiman et al., 2008) (see schematic in Figure 7A) that express EGFP-tagged ribosomal protein L10a (Rpl10a) driven by cell type-specific transgene promoters in motor neurons (Chat-bacTRAP), astrocytes (Aldh1l1-bacTRAP), or oligodendrocytes (Cnp1-bacTRAP) (Doyle et al., 2008; Heiman et al., 2008). Analysis of affinity-isolated, actively translating, polyribosome-associated mRNAs from each cell type (Figure 7B) revealed that translating MIF mRNA was found in all three cell types, with motor neurons accumulating the highest level (Figure 7C). Thus, MIF is synthesized actively by motor neurons, and its low accumulation in motor neuron cell bodies (Figure 6) must be the result of rapid clearance (secretion, degradation, or transport) from the perikarya of those neurons.

Increased MIF Enhances Survival of Mutant SOD1-Expressing Motor Neurons

To test whether increased synthesis and accumulation of MIF could be protective of mutant SOD1-expressing motor neurons, motor neurons were isolated by fluorescence-activated cell sorting (FACS) for expression of an HB9-promoted GFP motor neuron reporter gene following differentiation from nontransgenic (non-Tg) mouse embryonic stem cells or induced pluripotent stem cells (iPSCs) derived from mice expressing human wild-type (SOD1[WT]) or mutant (SOD1[G93A]) SOD1 transgenes (see schematic in Figure 8A). MIF synthesis was elevated by transduction with a lentivirus (Lv) encoding MIF and red fluorescent protein (RFP) (the latter translated from an internal ribosomal entry site in the MIF 3′ UTR). Beginning day 3 posttransduction, intraneuronal levels of MIF (detected by indirect immunofluorescence with MIF antibody) were elevated relative to motor neurons transduced with RFP alone (Figure 8B). The contrast between the failure of endogenously synthesized MIF to accumulate in mature motor neurons (Figure 6) and its accumulation via lentiviral transduction in cultured motor neurons (Figure 8) can be explained in two ways. Elevated MIF synthesis in cultured motor neurons may saturate degradation or secretion machineries. Alternatively, the degradation/secretion of endogenous MIF in mature motor neurons may reflect a non-cell-autonomous influence, especially on secretion, exercised by the partner glial cells, which are missing in our pure neuronal cultures.

Direct live-cell imaging (Figure 8C) revealed that, compared to nontransgenic or SOD1[WT] motor neurons, only one-fifth as many mutant SOD1[G93A]-expressing motor neurons survived the first 2 days of culture prior to MIF synthesis (Figures 8D–8F). MIF expression, however, significantly attenuated this accelerated motor neuron death at subsequent time points (Figure 8F).
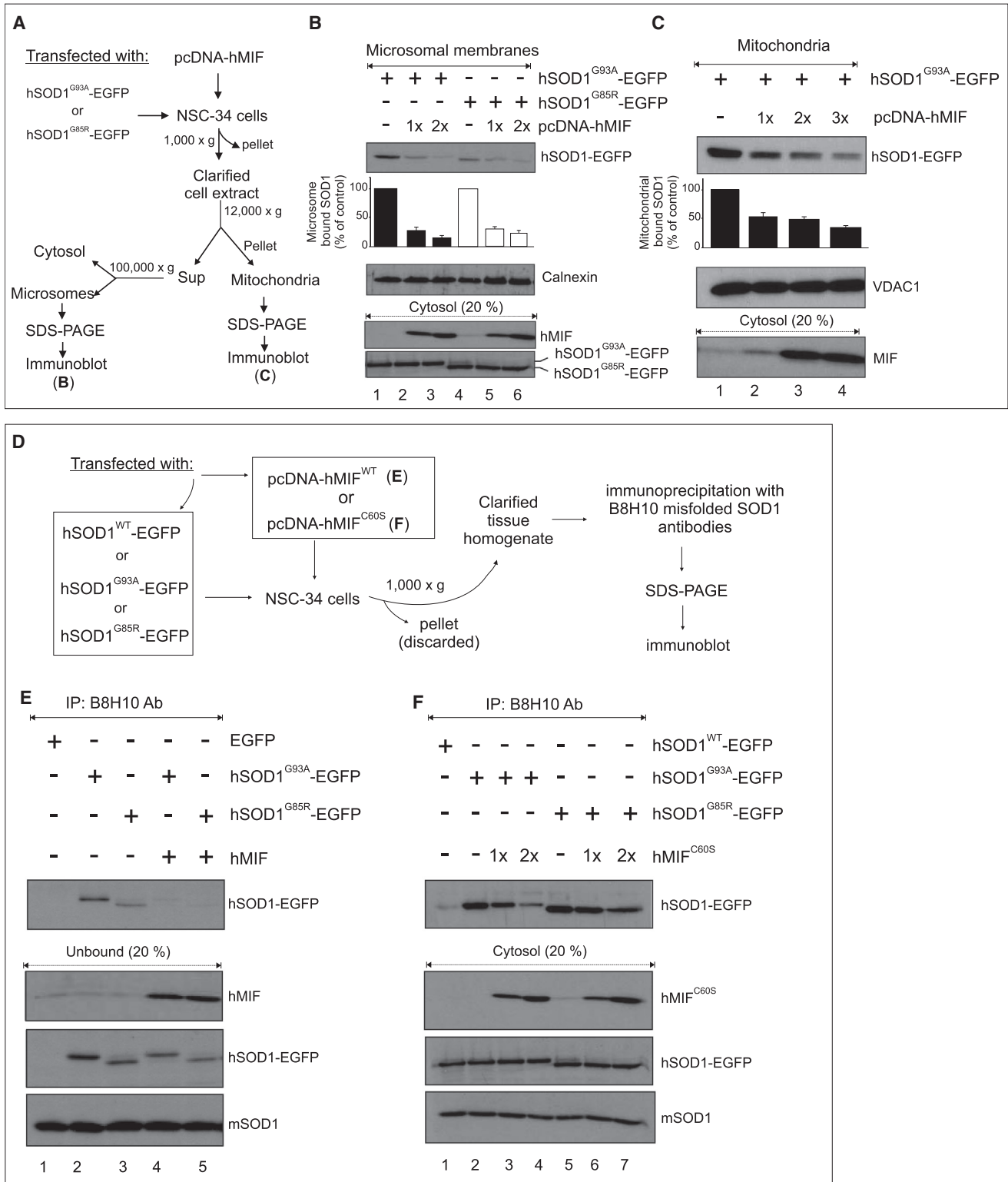
Figure 4. MIF Inhibits the Association of Misfolded Mutant SOD1 with Intracellular Membranes in a Cell-Culture Model of ALS

(A) Schematic of a protocol for assaying MIF-dependent inhibition of mutant SOD1 association in vivo with microsomes or mitochondria following expression of MIF and SOD1[G85R] or SOD1[G93A] in motor neuron-like NSC-34 cells.

(legend continued on next page)

Similarly, increased MIF significantly increased neurite length of the surviving SOD1^{G93A} motor neurons (Figure 8G).

DISCUSSION

Among the important unsolved questions in the disease mechanism from ubiquitous expression of mutant SOD1 is what determines the selective, age-dependent motor neuronal degeneration that is accompanied by mutant SOD1 misfolding and its association with mitochondria and the ER. We have now determined that both dismutase active and inactive SOD1 mutant association with such organelles can be suppressed by cytosolic MIF acting catalytically to inhibit misfolded SOD1 accumulation and its association with mitochondria and the ER. Furthermore, increased MIF, which normally accumulates only to low levels within the cell bodies of motor neurons, suppresses misfolded SOD1 accumulation and extends mutant SOD1-expressing motor neuron survival in cell culture. The low level of MIF accumulated within motor neurons correlates with accumulation of misfolded SOD1 species and their association with different intracellular organelles within those neurons.

Despite its small size (12 kDa), MIF has previously been implicated in both extracellular and intracellular roles. MIF was one of the first cytokines to be described (George and Vaughan, 1962), with its action in the immune response upstream of tumor necrosis factor-α, interleukin-1β, interferon-γ, and other effector cytokines (Calandra and Roger, 2003). MIF is synthesized as a cytoplasmic protein (a point we have validated after removal of even small vesicles from extracts of peripheral and nervous system tissues; Figure 2E), with cytokine activity achieved by posttranslational sequestration of cytoplasmic MIF into vesicles for release by an as yet unidentified mechanism in response to a variety of signals (Merk et al., 2009).

Intracellularly, MIF acts as a chaperone protein (Cherepkova et al., 2006) and a thiol-protein oxidoreductase (Kleemann et al., 1998). Its protein folding activity derives from switching from multimeric to monomeric forms, thereby exposing a hydrophobic surface that can provide ATP-independent chaperone activity. MIF's multiple activities parallel the well-known ATP-dependent protein chaperone Hsp70, for which dual roles as a chaperone and cytokine have also been reported (Asea et al., 2000; Pockley et al., 2009). The ability of MIF to act as a thiol-protein oxidoreductase was initially of special interest to us for four primary reasons. First, a major portion of misfolded SOD1 has been proposed to be composed of SOD1 monomers lacking the C57-C146 disulfide bond (Zetterström et al., 2013). Second, mutant SOD1 proteins that associate with mitochondria have been reported to be partially oxidized (Ferri et al., 2006), and Cys-111 was reported to be necessary for mutant SOD1 association with mitochondria (Cozzolino et al., 2008; Ferri et al., 2006). Third, thiol-reductase activity has been proposed to reduce oxidative stress and inhibit apoptosis (Nguyen et al., 2003). Finally, overexpression of glutaredoxin-1 or glutaredoxin-2, each with thiol-oxidoreductase activity, was reported to improve the solubility of the mutant SOD1 and to prevent its mitochondrial binding (Cozzolino et al., 2008; Ferri et al., 2010). Nevertheless, using a MIF mutant that lacks all thiol-oxidoreductase activity, we have demonstrated that it is the chaperone, not thiol-oxidoreductase, activity of MIF that can inhibit mutant SOD1 misfolding and membrane association.

We would also note that nearly eliminating aggregated misfolded SOD1 (by increasing mitochondrial buffering of calcium by deletion of cyclophilin-D) has no effect on ameliorating fatal disease progression in multiple SOD1 mutant mouse models (Parone et al., 2013). Hence, rather than highly aggregated forms as the toxic species, in vivo toxicity appears to derive from soluble, misfolded SOD1, which remained unaffected in mice with reduced aggregated mutant SOD1. This is the SOD1 species that we have shown that MIF chaperone activity acts to reduce. Other chaperones previously linked to SOD1, including Hsp27, aB-crystallin, and Hsc70, were unable to suppress mutant SOD1 binding to mitochondria or accumulation of newly formed misfolded SOD1. From these collective efforts, we now propose that low MIF chaperone-like activity in alpha motor neurons plays a pivotal role in misfolded SOD1 accumulation and subsequent toxicity.

Of relevance to MIF's extracellular activities, mutant SOD1 synthesized by microglia drives rapid disease progression (Beers et al., 2006; Boillée et al., 2006). Additionally, immunodeficiency shortened mutant SOD1 mouse lifespan (Beers et al., 2008; Chiu et al., 2008) whereas, conversely, passive transfer of activated T regulatory cells to immunocompetent mice modestly extended survival (Beers et al., 2011). We note that one of the manifestations of immune deficits in ALS could be a malfunction of MIF, thereby leading to accumulation of soluble misfolded SOD1 and binding to intracellular targets. Indeed, recognizing the potential for cell-to-cell spread of misfolded SOD1 as a means of disease propagation (Grad and Cashman, 2014; Grad et al., 2011; Münch et al., 2011), chaperone activity by extracellular MIF may act to limit such spreading.

(B and C) Immunoblots for mutant SOD1 associated with (B) microsomes or (C) mitochondria purified from NSC-34 cells transfected to express mutant SOD1^{G93A} or SOD1^{G85R} and low or high levels of MIF. Parallel immunoblotting for calnexin or VDAC1 was used to verify comparable recovery of microsomes or mitochondria, respectively. Similar immunoblot analyses of the initial cytosols were used to determine initial accumulated levels of MIF and mutant SOD1. Bar values represent the means ± SEM of three independent experiments.

(D) Schematic of protocol to test whether expression of MIF, with or without its thiol-oxidoreductase activity, can act in vivo to suppress accumulation of misfolded mutant SOD1 within NSC-34 cells.

(E and F) MIF was expressed by transient transfection in NSC-34 motor neuron-like cells also transfected to express wild-type or mutant human SOD1. Misfolded SOD1 was detected by immunoblotting of immunoprecipitates produced with the B8H10 antibody, which recognizes epitopes within exon 3 that are buried in correctly folded SOD1. IP, immunoprecipitation.

(E) Expression of wild-type MIF.

(F) Expression of MIF^{C60S} lacking thiol-oxidoreductase activity. MIF, endogenous SOD1, and EGFP-tagged wild-type or mutant human SOD1 levels were determined by immunoblotting in the unbound or initial cytosol fractions.
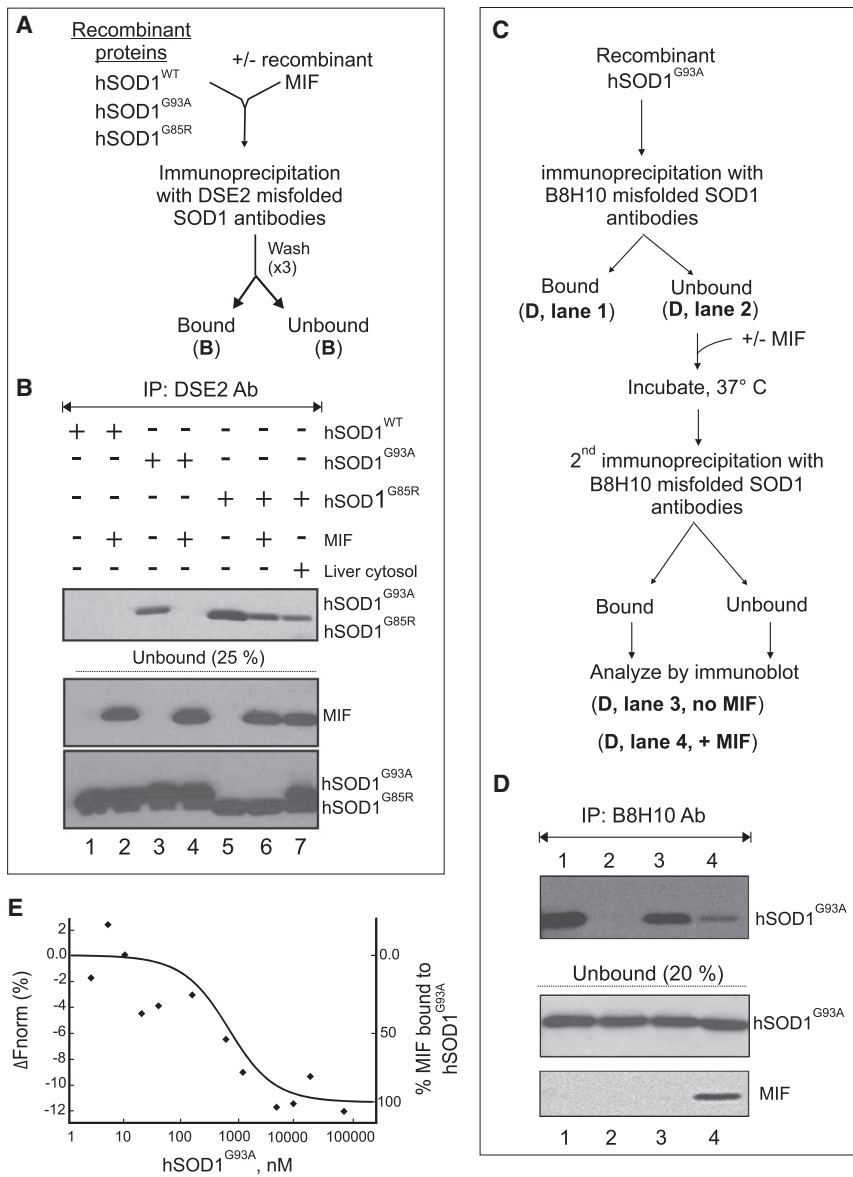
Figure 5. MIF Suppresses Misfolded Mutant SOD1 Accumulation by Directly Acting on It

(A) Protocol to determine whether purified recombinant MIF suppresses accumulation of misfolded SOD1 detectable with the DSE2 antibody, which recognizes an epitope in the electrostatic loop of hSOD1 (between residues 125 and 142) that is buried in correctly folded SOD1.

(B) Accumulation of misfolded SOD1 was determined by immunoblotting of immunoprecipitates with the DSE2 antibody after incubation of recombinant hSOD1 wild-type, hSOD1^{G93A}, or hSOD1^{G85R} (4 μg) in the absence or presence of recombinant MIF (100 ng). Immunoblotting was used to determine MIF levels remaining in the unbound fraction of each immunoprecipitation assay.

(C) Protocol to determine whether purified recombinant MIF suppresses accumulation of newly formed, misfolded SOD1 detectable with the B8H10 antibody for misfolded SOD1.

(D) Misfolded SOD1 determined by immunoblotting of immunoprecipitates of recombinant hSOD1^{G93A} with the B8H10 antibody (lane 1). The unbound fraction was subjected to a second immunoprecipitation performed immediately (lane 2) or after a 5-hr incubation in the (lane 3) absence or (lane 4) presence of recombinant MIF. Immunoblotting was also used to determine MIF levels remaining in the unbound fraction of each immunoprecipitation assay.

(E) Assay of MIF binding to mutant SOD1. Purified MIF (200 nM) was fluorescently labeled and incubated for 20 min at room temperature with increasing concentrations (from 2.4 nM to 80 μM) of SOD1^{G93A}. Closed diamonds indicate binding of MIF to SOD1^{G93A} determined by microscale thermophoresis assay. The smooth curve represents the predicted binding of MIF to mutant SOD1 calculated by curve fitting with a K_d of 367 nM (see Jerabek-Willemsen et al., 2011; Parker and Newstead, 2014; Wienken et al., 2010).

Finally, misfolded SOD1 has been reported by several groups to accumulate in motor neurons or glia in sporadic ALS (Bosco et al., 2010; Forsberg et al., 2010, 2011; Grad et al., 2014; Guareschi et al., 2012; Kabashi et al., 2007; Pokrishevsky et al., 2012; Zetterström et al., 2011a), although other efforts have reached opposite conclusions (Ayers et al., 2014; Brotherton et al., 2012; Kerman et al., 2010; Liu et al., 2009). Astrocytes generated from neuronal progenitor cells (NPCs) isolated from spinal cords of sporadic ALS patients have been found to be toxic to cocultured motor neurons (Haidet-Phillips et al., 2011), similar to what had been seen previously for astrocytes expressing mutant SOD1 (Di Giorgio et al., 2007; Marchetto et al., 2008; Nagai et al., 2007). Surprisingly, reducing wild-type SOD1 with small hairpin RNA significantly reduced toxicity to motor neurons of most of the "sporadic" ALS astrocytes (Haidet-Phillips et al., 2011), a finding directly disputed by others who concluded that wild-type SOD1 plays no role in the toxicity of sporadic ALS-derived astrocytes (Re et al., 2014).

The controversy notwithstanding, misfolded protein accumulation is central to essentially all instances of inherited and sporadic ALS. Identification of MIF as an intracellular chaperone that stimulates folding/refolding of misfolded SOD1 suggests a new avenue for therapy development in ALS through increasing intracellular MIF levels. Combined with recognition that extracellular MIF is an inducer of metalloproteinase 9 (MMP9) (Yu et al., 2007), a component contributing to the selectivity of motor neuron vulnerability to SOD1 mutant-mediated death (Kaplan et al., 2014), this finding underscores how approaches to increasing intracellular MIF (e.g., by reducing its clearance from motor neurons) and/or to inhibiting its induction of MMP9 (e.g., with drugs that block MIF's interaction with its known receptor [CD74; Bai et al., 2012]) could be attractive therapeutic strategies.
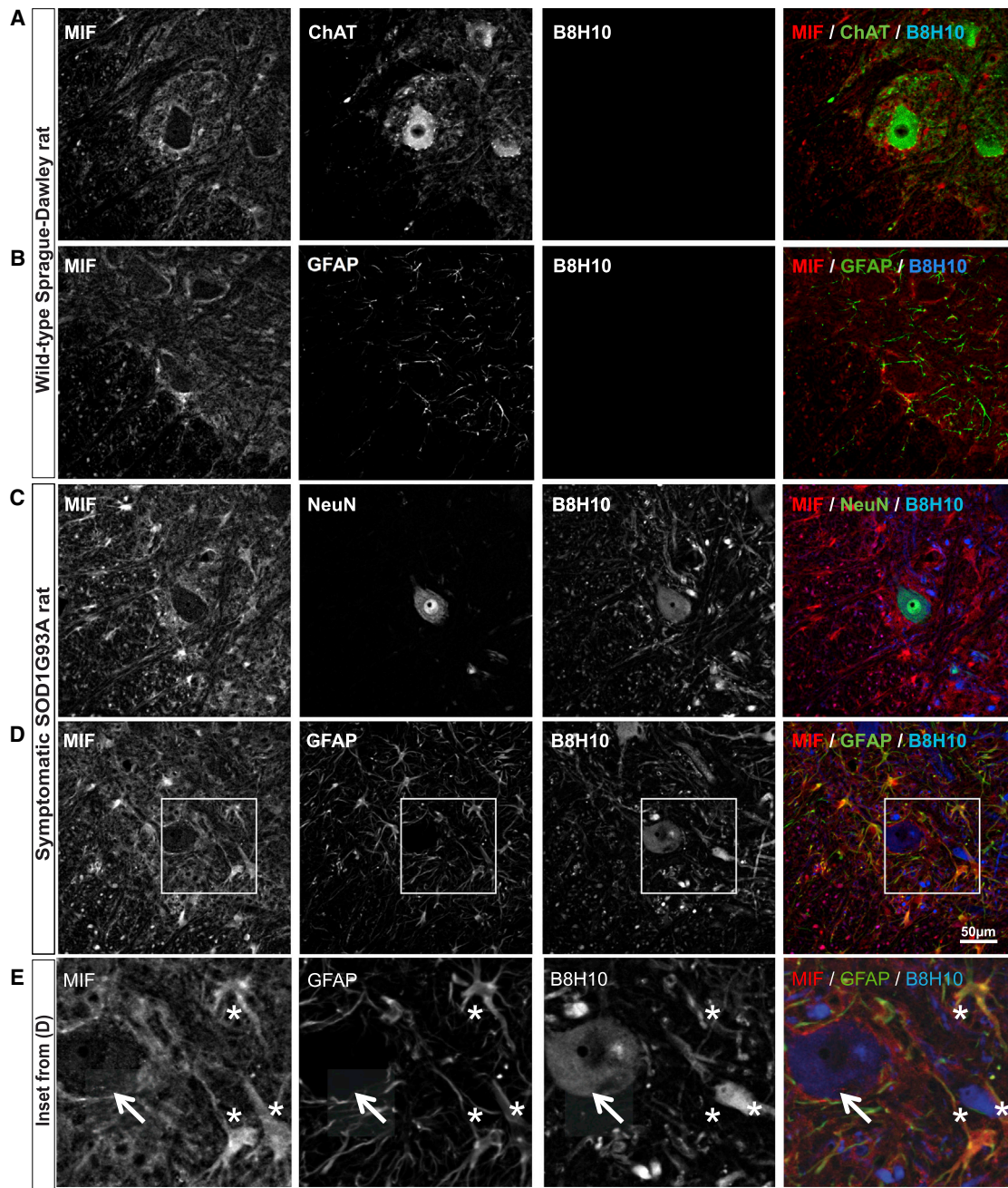
Figure 6. A Low Level of MIF in Motor Neuron Cell Bodies Is Accompanied by Diffuse Accumulation of Misfolded SOD1 within Those Cell Bodies Just after Disease Onset in SOD1^{G93A} Rats

(A) Accumulation of MIF in lumbar spinal cord of a nontransgenic rat assayed by indirect immunofluorescence with antibodies to MIF along with simultaneous identification of motor neurons (with antibodies to ChAT) and misfolded SOD1 (with the B8H10 antibody).

(B) An analogous assay as in (A) but with astrocytes identified with an antibody to glial fibrillary acidic protein (GFAP).

(C) Accumulation of MIF in lumbar spinal cord of an early symptomatic SOD1^{G93A} rat, 1 week after the first spontaneous muscle fibrillation, along with simultaneous identification of motor neurons (identified by morphology, position, and antibodies to NeuN) and misfolded SOD1 (with the B8H10 antibody).

(D) An analogous assay as in (C) but with astrocytes identified with an antibody to GFAP. The scale bar represents 50 μm.

(E) Higher magnification of the insets outlined in (D). The arrows highlight a motor neuron lacking MIF immunostaining, and asterisks mark GFAP-positive astrocytes containing MIF.
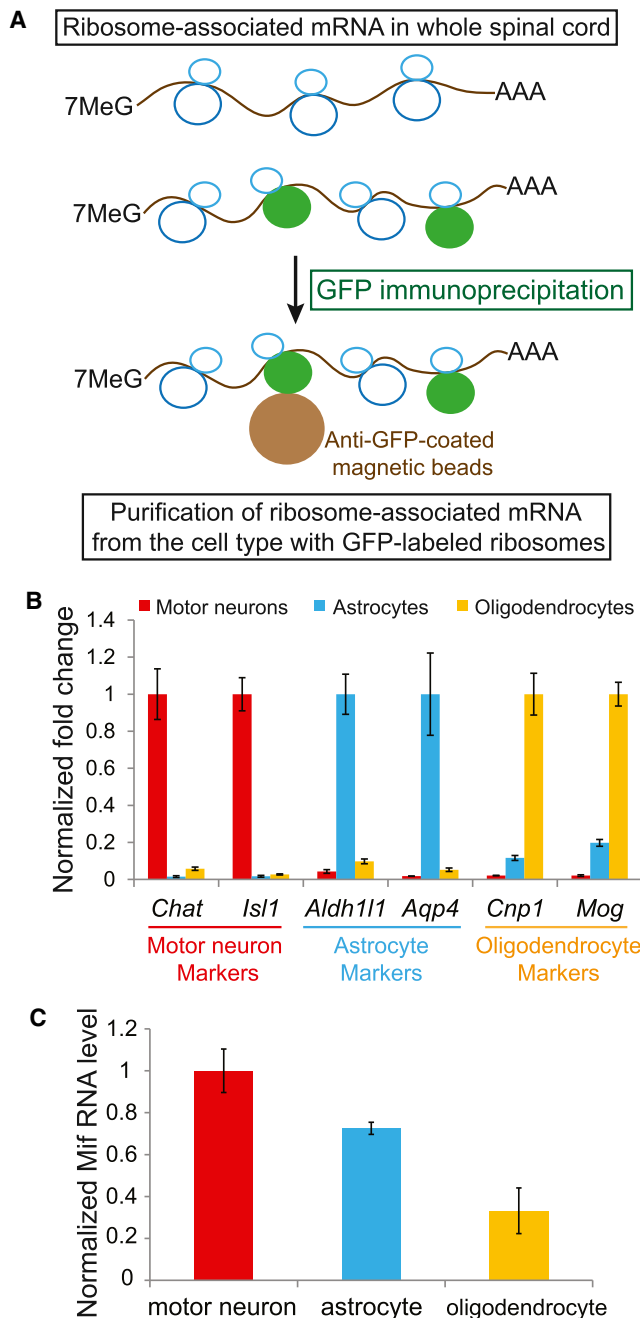
Figure 7. Translational mRNA Levels of MIF in Specific Cell Types in Mouse Spinal Cord
(A) Schematic of the bacTRAP methodology for isolating cell type-specific translated mRNAs.
(B) Relative RNA levels (assessed by qRT-PCR) of cell type-specific markers to test the efficacy of polysome-associated RNA purification from motor neurons, astrocytes, and oligodendrocytes.
(C) Relative MIF RNA level (assayed by qRT-PCR) of polysomal RNAs isolated from motor neurons, astrocytes, and oligodendrocytes. Levels are normalized to Dnaja2.
Error bars represent SEM from three or four biological replicates.

EXPERIMENTAL PROCEDURES

Transgenic Animals

Transgenic rats expressing hSOD1^{WT} (Chan et al., 1998), hSOD1^{G93A} (Howland et al., 2002), and hSOD1^{H46R} (Nagai et al., 2001) were as originally described. Transgenic mice expressing mutant SOD1^{G85R} (line 148), SOD1^{G37R} (line 42), or SOD1^{G93A} were maintained by standard protocols in the D.W.C. laboratory. bacTRAP transgenic mouse lines: *Chat*-bacTRAP line expresses EGFP-tagged ribosome protein Rpl10a only within motor neurons. The *Aldh1l1*-bacTRAP line expresses the same EGFP-tagged Rpl10a in astrocytes, whereas the *Cnp1*-bacTRAP line expresses in mature oligodendrocytes (Doyle et al., 2008; Heiman et al., 2008). All animal procedures were consistent with the requirements of the Animal Care and Use Committees of the University of California and Ben-Gurion University of the Negev.

Mutant SOD1 Binding to Mitochondria

Spinal cord or liver cytosolic fractions (200 μg) from hSOD1^{G93A} (~90-d-old) or hSOD1^{H46R} (~200-d-old) symptomatic female rats or recombinant hSOD1^{WT}, hSOD1^{G93A}, or hSOD1^{G85R} proteins (4 μg) were incubated with spinal cord or liver mitochondria (50 μg) isolated from nontransgenic rats for 30 min at 37°C in the presence or absence of recombinant mouse MIF (R&D Systems) at the indicated concentration. Where indicated, recombinant mutant SOD1 was incubated with proteinase K (100 μg/ml) for 15 min. The reaction was stopped by addition of 10 mM PMSF followed by incubation on ice for 10 min. Then, the mitochondrial fraction was recovered by centrifugation at 12,000 × g for 10 min at 4°C and washed twice with mitochondrial buffer. The pellet was resuspended with sample buffer and run on SDS-PAGE.

iPSC Generation

Neuronal progenitor cells expressing the motor neuron HB9::GFP reporter obtained from SOD1^{WT} and SOD1^{G93A} mice were converted to iPSCs. As previously described, retrovirus encoding OCT3/4 and KLF4 was sufficient to generate iPSC clones (Hester et al., 2009; Kim et al., 2008). Twenty viral particles per cell were needed to efficiently reprogram the cells. Cells were cultured in the presence of NPC media for 4 days followed by a change to mouse embryonic stem cell (mESC) media with DMEM (Millipore), supplemented with ES fetal bovine serum (18%; Invitrogen), L-glutamine (2 mM; Invitrogen), nonessential amino acids (1×; Millipore), antibiotic-antimycotic (1%; Invitrogen), 2-mercaptoethanol (114 μM; Sigma), and recombinant LIF (100 U/ml; Millipore). iPSC clones were morphologically similar to mouse ESCs (HBG3 cells; Thomas Jessell, Columbia University) and were obtained within 2 weeks. A wide panel of markers was used to compare ESCs with the newly generated iPSC lines and found no significant difference in their expression between cell lines.

Mouse Motor Neuron Differentiation

Mouse ESCs or iPSCs expressing HB9::GFP reporter were cultured on top of inactivated mouse fibroblasts (Millipore). Motor neuron differentiation was induced by plating 1–2 × 10^6 mES cells per 10-cm dish in the presence of 2 μM retinoic acid (Sigma-Aldrich) and 2 μM purmorphamine (Calbiochem). After 5 days of differentiation, embryonic bodies were dissociated and sorted based on levels of GFP using a FACSVantage/DiVa sorter (BD Biosciences).

Expression of MIF in Mouse Motor Neurons and Analysis

To express MIF in motor neurons, a previously described protocol was followed with minor modifications (Kaech and Banker, 2006). Briefly, sorted GFP$^+$ motor neurons were plated at a density of 15,000 cells per well on a laminin-coated 96-well plate. Twelve hours after plating, the cells were infected with lentivirus to overexpress transgenes (40 viral particles per motor neuron). Motor neuron cultures were allowed to continue for another 5 days, with half of the media being replaced every other day. RFP could be detected after 72 hr postinfection. At various time points during the culture of motor neurons, images were recorded using a fully automated IN Cell 6000 cell imager (GE Healthcare) as previously reported (Meyer et al., 2014). Images were further processed with the Developer and Analyzer software package (GE Healthcare) for survival counts and neurite length measurements. Unless otherwise noted,
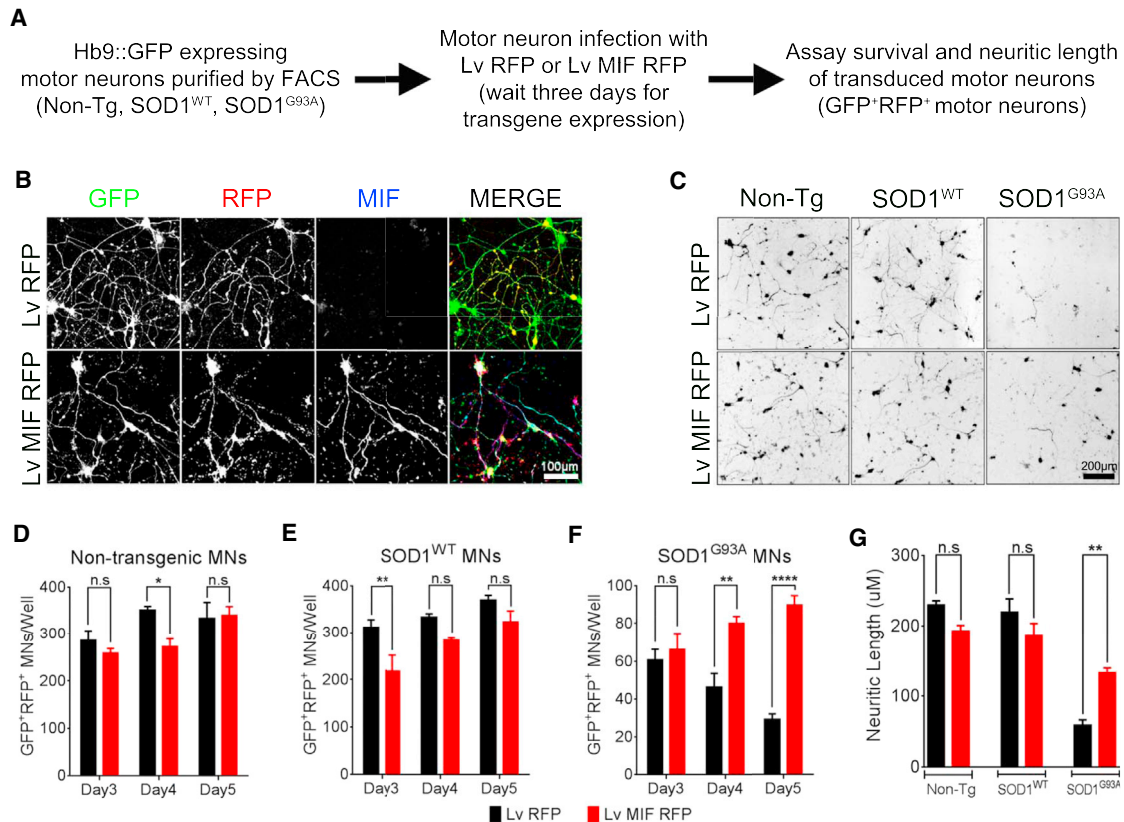
Figure 8. Increased Accumulation of MIF Enhances Survival of Primary Motor Neurons Expressing Mutant SOD1

(A) Protocol for generating motor neurons and assaying effects of MIF expression.

(B) Representative images of motor neuron cultures at 96 hr postinfection with Lv-RFP or Lv-MIF-RFP and using immunocytochemistry to reveal human MIF and RFP in motor neurons.

(C–F) Viability of GFP[+]RFP[+] nontransgenic, SOD1[WT], and SOD1[G93A] motor neurons (MNs) (C) imaged at 5 days or (D–F) quantified from images taken from 3 to 5 days after transduction with lentivirus encoding RFP or MIF and RFP. Data are representative of three independent experiments and are displayed as the mean ± SEM counts of triplicate wells. Two-way ANOVA was used for statistical analysis. *$p < 0.05$; **$p < 0.01$; ****$p < 0.0001$; n.s, nonsignificant.

(G) Neurite length measurements quantified from images as in (C) taken at day 5. Data show a representative example of two independent experiments and are displayed as the median with range. One hundred neurites per condition were included for measurements. Student's t test was used for statistical analysis. **$p < 0.01$; n.s, nonsignificant.

images shown represent 120 hr postinfection. All counts were performed in triplicate and repeated at least three times.

REFERENCES

Asea, A., Kraeft, S.K., Kurt-Jones, E.A., Stevenson, M.A., Chen, L.B., Finberg, R.W., Koo, G.C., and Calderwood, S.K. (2000). HSP70 stimulates cytokine production through a CD14-dependant pathway, demonstrating its dual role as a chaperone and cytokine. Nat. Med. 6, 435–442.

Ayers, J.I., Xu, G., Pletnikova, O., Troncoso, J.C., Hart, P.J., and Borchelt, D.R. (2014). Conformational specificity of the C4F6 SOD1 antibody; low frequency of reactivity in sporadic ALS cases. Acta Neuropathol. Commun. 2, 55.

Bai, F., Asojo, O.A., Cirillo, P., Ciustea, M., Ledizet, M., Aristoff, P.A., Leng, L., Koski, R.A., Powell, T.J., Bucala, R., and Anthony, K.G. (2012). A novel

allosteric inhibitor of macrophage migration inhibitory factor (MIF). J. Biol. Chem. *287*, 30653–30663.

Beers, D.R., Henkel, J.S., Xiao, Q., Zhao, W., Wang, J., Yen, A.A., Siklos, L., McKercher, S.R., and Appel, S.H. (2006). Wild-type microglia extend survival in PU.1 knockout mice with familial amyotrophic lateral sclerosis. Proc. Natl. Acad. Sci. USA *103*, 16021–16026.

Beers, D.R., Henkel, J.S., Zhao, W., Wang, J., and Appel, S.H. (2008). CD4+ T cells support glial neuroprotection, slow disease progression, and modify glial morphology in an animal model of inherited ALS. Proc. Natl. Acad. Sci. USA *105*, 15558–15563.

Beers, D.R., Henkel, J.S., Zhao, W., Wang, J., Huang, A., Wen, S., Liao, B., and Appel, S.H. (2011). Endogenous regulatory T lymphocytes ameliorate amyotrophic lateral sclerosis in mice and correlate with disease progression in patients with amyotrophic lateral sclerosis. Brain *134*, 1293–1314.

Boillée, S., Yamanaka, K., Lobsiger, C.S., Copeland, N.G., Jenkins, N.A., Kassiotis, G., Kollias, G., and Cleveland, D.W. (2006). Onset and progression in inherited ALS determined by motor neurons and microglia. Science *312*, 1389–1392.

Borchelt, D.R., Lee, M.K., Slunt, H.S., Guarnieri, M., Xu, Z.S., Wong, P.C., Brown, R.H., Jr., Price, D.L., Sisodia, S.S., and Cleveland, D.W. (1994). Superoxide dismutase 1 with mutations linked to familial amyotrophic lateral sclerosis possesses significant activity. Proc. Natl. Acad. Sci. USA *91*, 8292–8296.

Bosco, D.A., Morfini, G., Karabacak, N.M., Song, Y., Gros-Louis, F., Pasinelli, P., Goolsby, H., Fontaine, B.A., Lemay, N., McKenna-Yasek, D., et al. (2010). Wild-type and mutant SOD1 share an aberrant conformation and a common pathogenic pathway in ALS. Nat. Neurosci. *13*, 1396–1403.

Brotherton, T.E., Li, Y., Cooper, D., Gearing, M., Julien, J.P., Rothstein, J.D., Boylan, K., and Glass, J.D. (2012). Localization of a toxic form of superoxide dismutase 1 protein to pathologically affected tissues in familial ALS. Proc. Natl. Acad. Sci. USA *109*, 5505–5510.

Calandra, T., and Roger, T. (2003). Macrophage migration inhibitory factor: a regulator of innate immunity. Nat. Rev. Immunol. *3*, 791–800.

Chan, P.H., Kawase, M., Murakami, K., Chen, S.F., Li, Y., Calagui, B., Reola, L., Carlson, E., and Epstein, C.J. (1998). Overexpression of SOD1 in transgenic rats protects vulnerable neurons against ischemic damage after global cerebral ischemia and reperfusion. J. Neurosci. *18*, 8292–8299.

Cherepkova, O.A., Lyutova, E.M., Eronina, T.B., and Gurvits, B.Y. (2006). Chaperone-like activity of macrophage migration inhibitory factor. Int. J. Biochem. Cell Biol. *38*, 43–55.

Chiu, I.M., Chen, A., Zheng, Y., Kosaras, B., Tsiftsoglou, S.A., Vartanian, T.K., Brown, R.H., Jr., and Carroll, M.C. (2008). T lymphocytes potentiate endogenous neuroprotective inflammation in a mouse model of ALS. Proc. Natl. Acad. Sci. USA *105*, 17913–17918.

Cozzolino, M., Amori, I., Pesaresi, M.G., Ferri, A., Nencini, M., and Carrì, M.T. (2008). Cysteine 111 affects aggregation and cytotoxicity of mutant Cu,Zn-superoxide dismutase associated with familial amyotrophic lateral sclerosis. J. Biol. Chem. *283*, 866–874.

Da Cruz, S., and Cleveland, D.W. (2011). Understanding the role of TDP-43 and FUS/TLS in ALS and beyond. Curr. Opin. Neurobiol. *21*, 904–919.

Di Giorgio, F.P., Carrasco, M.A., Siao, M.C., Maniatis, T., and Eggan, K. (2007). Non-cell autonomous effect of glia on motor neurons in an embryonic stem cell-based ALS model. Nat. Neurosci. *10*, 608–614.

Doyle, J.P., Dougherty, J.D., Heiman, M., Schmidt, E.F., Stevens, T.R., Ma, G., Bupp, S., Shrestha, P., Shah, R.D., Doughty, M.L., et al. (2008). Application of a translational profiling approach for the comparative analysis of CNS cell types. Cell *135*, 749–762.

Ferri, A., Cozzolino, M., Crosio, C., Nencini, M., Casciati, A., Gralla, E.B., Rotilio, G., Valentine, J.S., and Carrì, M.T. (2006). Familial ALS-superoxide dismutases associate with mitochondria and shift their redox potentials. Proc. Natl. Acad. Sci. USA *103*, 13860–13865.

Ferri, A., Fiorenzo, P., Nencini, M., Cozzolino, M., Pesaresi, M.G., Valle, C., Sepe, S., Moreno, S., and Carrì, M.T. (2010). Glutaredoxin 2 prevents aggrega-tion of mutant SOD1 in mitochondria and abolishes its toxicity. Hum. Mol. Genet. *19*, 4529–4542.

Forsberg, K., Jonsson, P.A., Andersen, P.M., Bergemalm, D., Graffmo, K.S., Hultdin, M., Jacobsson, J., Rosquist, R., Marklund, S.L., and Brännström, T. (2010). Novel antibodies reveal inclusions containing non-native SOD1 in sporadic ALS patients. PLoS ONE *5*, e11552.

Forsberg, K., Andersen, P.M., Marklund, S.L., and Brännström, T. (2011). Glial nuclear aggregates of superoxide dismutase-1 are regularly present in patients with amyotrophic lateral sclerosis. Acta Neuropathol. *121*, 623–634.

Freskgård, P.O., Bergenhem, N., Jonsson, B.H., Svensson, M., and Carlsson, U. (1992). Isomerase and chaperone activity of prolyl isomerase in the folding of carbonic anhydrase. Science *258*, 466–468.

Fujisawa, T., Homma, K., Yamaguchi, N., Kadowaki, H., Tsuburaya, N., Naguro, I., Matsuzawa, A., Takeda, K., Takahashi, Y., Goto, J., et al. (2012). A novel monoclonal antibody reveals a conformational alteration shared by amyotrophic lateral sclerosis-linked SOD1 mutants. Ann. Neurol. *72*, 739–749.

George, M., and Vaughan, J.H. (1962). In vitro cell migration as a model for delayed hypersensitivity. Proc. Soc. Exp. Biol. Med. *111*, 514–521.

Grad, L.I., and Cashman, N.R. (2014). Prion-like activity of Cu/Zn superoxide dismutase: implications for amyotrophic lateral sclerosis. Prion *8*, 33–41.

Grad, L.I., Guest, W.C., Yanai, A., Pokrishevsky, E., O'Neill, M.A., Gibbs, E., Semenchenko, V., Yousefi, M., Wishart, D.S., Plotkin, S.S., and Cashman, N.R. (2011). Intermolecular transmission of superoxide dismutase 1 misfolding in living cells. Proc. Natl. Acad. Sci. USA *108*, 16398–16403.

Grad, L.I., Yerbury, J.J., Turner, B.J., Guest, W.C., Pokrishevsky, E., O'Neill, M.A., Yanai, A., Silverman, J.M., Zeineddine, R., Corcoran, L., et al. (2014). Intercellular propagated misfolding of wild-type Cu/Zn superoxide dismutase occurs via exosome-dependent and -independent mechanisms. Proc. Natl. Acad. Sci. USA *111*, 3620–3625.

Gros-Louis, F., Soucy, G., Larivière, R., and Julien, J.P. (2010). Intracerebroventricular infusion of monoclonal antibody or its derived Fab fragment against misfolded forms of SOD1 mutant delays mortality in a mouse model of ALS. J. Neurochem. *113*, 1188–1199.

Guareschi, S., Cova, E., Cereda, C., Ceroni, M., Donetti, E., Bosco, D.A., Trotti, D., and Pasinelli, P. (2012). An over-oxidized form of superoxide dismutase found in sporadic amyotrophic lateral sclerosis with bulbar onset shares a toxic mechanism with mutant SOD1. Proc. Natl. Acad. Sci. USA *109*, 5074–5079.

Haidet-Phillips, A.M., Hester, M.E., Miranda, C.J., Meyer, K., Braun, L., Frakes, A., Song, S., Likhite, S., Murtha, M.J., Foust, K.D., et al. (2011). Astrocytes from familial and sporadic ALS patients are toxic to motor neurons. Nat. Biotechnol. *29*, 824–828.

Heiman, M., Schaefer, A., Gong, S., Peterson, J.D., Day, M., Ramsey, K.E., Suárez-Fariñas, M., Schwarz, C., Stephan, D.A., Surmeier, D.J., et al. (2008). A translational profiling approach for the molecular characterization of CNS cell types. Cell *135*, 738–748.

Hester, M.E., Song, S., Miranda, C.J., Eagle, A., Schwartz, P.H., and Kaspar, B.K. (2009). Two factor reprogramming of human neural stem cells into pluripotency. PLoS ONE *4*, e7044.

Howland, D.S., Liu, J., She, Y., Goad, B., Maragakis, N.J., Kim, B., Erickson, J., Kulik, J., DeVito, L., Psaltis, G., et al. (2002). Focal loss of the glutamate transporter EAAT2 in a transgenic rat model of SOD1 mutant-mediated amyotrophic lateral sclerosis (ALS). Proc. Natl. Acad. Sci. USA *99*, 1604–1609.

Ilieva, H., Polymenidou, M., and Cleveland, D.W. (2009). Non-cell autonomous toxicity in neurodegenerative disorders: ALS and beyond. J. Cell Biol. *187*, 761–772.

Israelson, A., Arbel, N., Da Cruz, S., Ilieva, H., Yamanaka, K., Shoshan-Barmatz, V., and Cleveland, D.W. (2010). Misfolded mutant SOD1 directly inhibits VDAC1 conductance in a mouse model of inherited ALS. Neuron *67*, 575–587.

Jerabek-Willemsen, M., Wienken, C.J., Braun, D., Baaske, P., and Duhr, S. (2011). Molecular interaction studies using microscale thermophoresis. Assay Drug Dev. Technol. *9*, 342–353.

Kabashi, E., Valdmanis, P.N., Dion, P., and Rouleau, G.A. (2007). Oxidized/misfolded superoxide dismutase-1: the cause of all amyotrophic lateral sclerosis? Ann. Neurol. 62, 553–559.

Kaech, S., and Banker, G. (2006). Culturing hippocampal neurons. Nat. Protoc. 1, 2406–2415.

Kaplan, A., Spiller, K.J., Towne, C., Kanning, K.C., Choe, G.T., Geber, A., Akay, T., Aebischer, P., and Henderson, C.E. (2014). Neuronal matrix metalloproteinase-9 is a determinant of selective neurodegeneration. Neuron 81, 333–348.

Karch, C.M., and Borchelt, D.R. (2010). An examination of alpha B-crystallin as a modifier of SOD1 aggregate pathology and toxicity in models of familial amyotrophic lateral sclerosis. J. Neurochem. 113, 1092–1100.

Kerman, A., Liu, H.N., Croul, S., Bilbao, J., Rogaeva, E., Zinman, L., Robertson, J., and Chakrabartty, A. (2010). Amyotrophic lateral sclerosis is a non-amyloid disease in which extensive misfolding of SOD1 is unique to the familial form. Acta Neuropathol. 119, 335–344.

Kim, J.B., Zaehres, H., Wu, G., Gentile, L., Ko, K., Sebastiano, V., Araúzo-Bravo, M.J., Ruau, D., Han, D.W., Zenke, M., and Schöler, H.R. (2008). Pluripotent stem cells induced from adult neural stem cells by reprogramming with two factors. Nature 454, 646–650.

Kleemann, R., Kapurniotu, A., Frank, R.W., Gessner, A., Mischke, R., Flieger, O., Jüttner, S., Brunner, H., and Bernhagen, J. (1998). Disulfide analysis reveals a role for macrophage migration inhibitory factor (MIF) as thiol-protein oxidoreductase. J. Mol. Biol. 280, 85–102.

Krishnan, J., Vannuvel, K., Andries, M., Waelkens, E., Robberecht, W., and Van Den Bosch, L. (2008). Over-expression of Hsp27 does not influence disease in the mutant SOD1(G93A) mouse model of amyotrophic lateral sclerosis. J. Neurochem. 106, 2170–2183.

Li, Q., Vande Velde, C., Israelson, A., Xie, J., Bailey, A.O., Dong, M.Q., Chun, S.J., Roy, T., Winer, L., Yates, J.R., et al. (2010). ALS-linked mutant superoxide dismutase 1 (SOD1) alters mitochondrial protein composition and decreases protein import. Proc. Natl. Acad. Sci. USA 107, 21146–21151.

Liu, J., Lillo, C., Jonsson, P.A., Vande Velde, C., Ward, C.M., Miller, T.M., Subramaniam, J.R., Rothstein, J.D., Marklund, S., Andersen, P.M., et al. (2004). Toxicity of familial ALS-linked SOD1 mutants from selective recruitment to spinal mitochondria. Neuron 43, 5–17.

Liu, H.N., Sanelli, T., Horne, P., Pioro, E.P., Strong, M.J., Rogaeva, E., Bilbao, J., Zinman, L., and Robertson, J. (2009). Lack of evidence of monomer/misfolded superoxide dismutase-1 in sporadic amyotrophic lateral sclerosis. Ann. Neurol. 66, 75–80.

Lolis, E., and Bucala, R. (2003). Macrophage migration inhibitory factor. Expert Opin. Ther. Targets 7, 153–164.

Marchetto, M.C., Muotri, A.R., Mu, Y., Smith, A.M., Cezar, G.G., and Gage, F.H. (2008). Non-cell-autonomous effect of human SOD1 G37R astrocytes on motor neurons derived from human embryonic stem cells. Cell Stem Cell 3, 649–657.

Mattiazzi, M., D'Aurelio, M., Gajewski, C.D., Martushova, K., Kiaei, M., Beal, M.F., and Manfredi, G. (2002). Mutated human SOD1 causes dysfunction of oxidative phosphorylation in mitochondria of transgenic mice. J. Biol. Chem. 277, 29626–29633.

Merk, M., Baugh, J., Zierow, S., Leng, L., Pal, U., Lee, S.J., Ebert, A.D., Mizue, Y., Trent, J.O., Mitchell, R., et al. (2009). The Golgi-associated protein p115 mediates the secretion of macrophage migration inhibitory factor. J. Immunol. 182, 6896–6906.

Meyer, K., Ferraiuolo, L., Miranda, C.J., Likhite, S., McElroy, S., Renusch, S., Ditsworth, D., Lagier-Tourenne, C., Smith, R.A., Ravits, J., et al. (2014). Direct conversion of patient fibroblasts demonstrates non-cell autonomous toxicity of astrocytes to motor neurons in familial and sporadic ALS. Proc. Natl. Acad. Sci. USA 111, 829–832.

Mischke, R., Kleemann, R., Brunner, H., and Bernhagen, J. (1998). Cross-linking and mutational analysis of the oligomerization state of the cytokine macrophage migration inhibitory factor (MIF). FEBS Lett. 427, 85–90.

Münch, C., O'Brien, J., and Bertolotti, A. (2011). Prion-like propagation of mutant superoxide dismutase-1 misfolding in neuronal cells. Proc. Natl. Acad. Sci. USA 108, 3548–3553.

Nagai, M., Aoki, M., Miyoshi, I., Kato, M., Pasinelli, P., Kasai, N., Brown, R.H., Jr., and Itoyama, Y. (2001). Rats expressing human cytosolic copper-zinc superoxide dismutase transgenes with amyotrophic lateral sclerosis: associated mutations develop motor neuron disease. J. Neurosci. 21, 9246–9254.

Nagai, M., Re, D.B., Nagata, T., Chalazonitis, A., Jessell, T.M., Wichterle, H., and Przedborski, S. (2007). Astrocytes expressing ALS-linked mutated SOD1 release factors selectively toxic to motor neurons. Nat. Neurosci. 10, 615–622.

Nguyen, M.T., Lue, H., Kleemann, R., Thiele, M., Tolle, G., Finkelmeier, D., Wagner, E., Braun, A., and Bernhagen, J. (2003). The cytokine macrophage migration inhibitory factor reduces pro-oxidative stress-induced apoptosis. J. Immunol. 170, 3337–3347.

Nishitoh, H., Kadowaki, H., Nagai, A., Maruyama, T., Yokota, T., Fukutomi, H., Noguchi, T., Matsuzawa, A., Takeda, K., and Ichijo, H. (2008). ALS-linked mutant SOD1 induces ER stress- and ASK1-dependent motor neuron death by targeting Derlin-1. Genes Dev. 22, 1451–1464.

Parker, J.L., and Newstead, S. (2014). Molecular basis of nitrate uptake by the plant nitrate transporter NRT1.1. Nature 507, 68–72.

Parone, P.A., Da Cruz, S., Han, J.S., McAlonis-Downes, M., Vetto, A.P., Lee, S.K., Tseng, E., and Cleveland, D.W. (2013). Enhancing mitochondrial calcium buffering capacity reduces aggregation of misfolded SOD1 and motor neuron cell death without extending survival in mouse models of inherited amyotrophic lateral sclerosis. J. Neurosci. 33, 4657–4671.

Pedrini, S., Sau, D., Guareschi, S., Bogush, M., Brown, R.H., Jr., Naniche, N., Kia, A., Trotti, D., and Pasinelli, P. (2010). ALS-linked mutant SOD1 damages mitochondria by promoting conformational changes in Bcl-2. Hum. Mol. Genet. 19, 2974–2986.

Philo, J.S., Yang, T.H., and LaBarre, M. (2004). Re-examining the oligomerization state of macrophage migration inhibitory factor (MIF) in solution. Biophys. Chem. 108, 77–87.

Pockley, A.G., Calderwood, S.K., and Multhoff, G. (2009). The atheroprotective properties of Hsp70: a role for Hsp70-endothelial interactions? Cell Stress Chaperones 14, 545–553.

Pokrishevsky, E., Grad, L.I., Yousefi, M., Wang, J., Mackenzie, I.R., and Cashman, N.R. (2012). Aberrant localization of FUS and TDP43 is associated with misfolding of SOD1 in amyotrophic lateral sclerosis. PLoS ONE 7, e35050.

Ratovitski, T., Corson, L.B., Strain, J., Wong, P., Cleveland, D.W., Culotta, V.C., and Borchelt, D.R. (1999). Variation in the biochemical/biophysical properties of mutant superoxide dismutase 1 enzymes and the rate of disease progression in familial amyotrophic lateral sclerosis kindreds. Hum. Mol. Genet. 8, 1451–1460.

Re, D.B., Le Verche, V., Yu, C., Amoroso, M.W., Politi, K.A., Phani, S., Ikiz, B., Hoffmann, L., Koolen, M., Nagata, T., et al. (2014). Necroptosis drives motor neuron death in models of both sporadic and familial ALS. Neuron 81, 1001–1008.

Rosen, D.R., Siddique, T., Patterson, D., Figlewicz, D.A., Sapp, P., Hentati, A., Donaldson, D., Goto, J., O'Regan, J.P., Deng, H.X., et al. (1993). Mutations in Cu/Zn superoxide dismutase gene are associated with familial amyotrophic lateral sclerosis. Nature 362, 59–62.

Vande Velde, C., Miller, T.M., Cashman, N.R., and Cleveland, D.W. (2008). Selective association of misfolded ALS-linked mutant SOD1 with the cytoplasmic face of mitochondria. Proc. Natl. Acad. Sci. USA 105, 4022–4027.

Vande Velde, C., McDonald, K.K., Boukhedimi, Y., McAlonis-Downes, M., Lobsiger, C.S., Bel Hadj, S., Zandona, A., Julien, J.P., Shah, S.B., and Cleveland, D.W. (2011). Misfolded SOD1 associated with motor neuron mitochondria alters mitochondrial shape and distribution prior to clinical onset. PLoS ONE 6, e22031.

Wang, J., Xu, G., Li, H., Gonzales, V., Fromholt, D., Karch, C., Copeland, N.G., Jenkins, N.A., and Borchelt, D.R. (2005). Somatodendritic accumulation of misfolded SOD1-L126Z in motor neurons mediates degeneration: alphaB-crystallin modulates aggregation. Hum. Mol. Genet. 14, 2335–2347.

Wang, J., Farr, G.W., Zeiss, C.J., Rodriguez-Gil, D.J., Wilson, J.H., Furtak, K., Rutkowski, D.T., Kaufman, R.J., Ruse, C.I., Yates, J.R., III., et al. (2009). Progressive aggregation despite chaperone associations of a mutant SOD1-YFP in transgenic mice that develop ALS. Proc. Natl. Acad. Sci. USA *106*, 1392–1397.

Wienken, C.J., Baaske, P., Rothbauer, U., Braun, D., and Duhr, S. (2010). Protein-binding assays in biological liquids using microscale thermophoresis. Nat. Commun. *1*, 100.

Wu, C.H., Fallini, C., Ticozzi, N., Keagle, P.J., Sapp, P.C., Piotrowska, K., Lowe, P., Koppers, M., McKenna-Yasek, D., Baron, D.M., et al. (2012). Mutations in the profilin 1 gene cause familial amyotrophic lateral sclerosis. Nature *488*, 499–503.

Yerbury, J.J., Gower, D., Vanags, L., Roberts, K., Lee, J.A., and Ecroyd, H. (2013). The small heat shock proteins αB-crystallin and Hsp27 suppress SOD1 aggregation in vitro. Cell Stress Chaperones *18*, 251–257.

Yu, X., Lin, S.G., Huang, X.R., Bacher, M., Leng, L., Bucala, R., and Lan, H.Y. (2007). Macrophage migration inhibitory factor induces MMP-9 expression in macrophages via the MEK-ERK MAP kinase pathway. J. Interferon Cytokine Res. *27*, 103–109.

Zetterström, P., Andersen, P.M., Brännström, T., and Marklund, S.L. (2011a). Misfolded superoxide dismutase-1 in CSF from amyotrophic lateral sclerosis patients. J. Neurochem. *117*, 91–99.

Zetterström, P., Graffmo, K.S., Andersen, P.M., Brännström, T., and Marklund, S.L. (2011b). Proteins that bind to misfolded mutant superoxide dismutase-1 in spinal cords from transgenic amyotrophic lateral sclerosis (ALS) model mice. J. Biol. Chem. *286*, 20130–20136.

Zetterström, P., Graffmo, K.S., Andersen, P.M., Brännström, T., and Marklund, S.L. (2013). Composition of soluble misfolded superoxide dismutase-1 in murine models of amyotrophic lateral sclerosis. Neuromolecular Med. *15*, 147–158.